Centering Responsive Navigation based on Motion Energy

Vincent Agerbech, Allan Johansen & Brian Johansen

Aalborg Media Lab, Aalborg University Copenhagen
Group 783, Semester 7, Medialogy 2004

Supervisor: Volker Krüger

February 28, 2005

Abstract

In this project we will try to simulate the self centering responds of insects using a robot as a testing platform. The robot will use motion energy calculations navigate.
The approach will be biological inspired. We will strive to understand the motion sensitive visual system of a fly. The reason for using the fly as an inspiration derives from the biological simplicity of its motion perception and its reaction to different visual stimulus.
Research with flies has led to an understanding within many of its connections between the visual system and the motor functions. This research is going to be a guiding inspiration for developing the centering responds of an autonomous robot vehicle. We will conduct experiments for two different approaches to the same problem, but with a primary focus on motion energy.

This project will cover the interesting apects of the fly's visual system. An understanding of this will lead to the perception of motion and how the motion energy solution is derived through this understanding.

Contents

Chapter 1

Introduction

This project is developed under the theme *merging of senses*. The project comes with a solution to centering responsive navigation applied to a robot. The reason for utilizing a robot is based on that it provides a hardware platform for testing derived solutions, with instantaneous feedback. Instantaneous feedback is important, because when navigating in a testing environment problems often occur. Problems can be in the form of illumination problems or that the robot drives into a wall for no apparent reason. These occurrences give thought for improvements and new solutions.

As stated above, this project comes with a solution to centering responsive navigation. This is obtained through *Motion Energy*. So what is Motion Energy? Motion Energy is the calculation of non-directional optical flow, where motion energy on the left and the right side of the robot are compared. This comparison is evaluated to determine the direction of the robot. This solution has been derived through thorough investigation of the visual system of the fly and research within the field of robot navigation inspired by the insects.

The robots visual system on which the Motion Energy solution was applied originated from the eye of the fly. The visual system where the visual input is derived from is created by utilizing a reflective sphere. Even though it in its form isn't as precise as the fly's eye it works well with Motion Energy processing.

In our experiments with the robot using Centering Responsive Navigation based on Motion Energy, it performed well, but also as expected with an oscillating behavior. Even though it oscillated a lot, it still showed a centering response to the Motion Energy input in its visual field.

Utilizing one sense, the visual sense; the robot performed well, but the project should have incorporated two or more in order to for fill the theme of *merging of senses*. This was discarded due to the satisfactory results of our experiments.

Chapter 2

Visual navigation in flying insects

2.1 Discovering optical flow in flies

In 1891 Exner was the first to speculate that invertebrates use image motion to estimate object range, but not before 1959 G. K. Wallace observed that locust sway there head from side to side before jumping. Through a range of tests, Wallaces conclusion was that this peering behavior was to measure object range. Exners and Wallaces research was groundbreaking because they were the first to link an insect's vision to image motion. Wallaces research was not unambiguous, not all insects use peering to measure object range. Insects in locomotion are not able to perform this peering behavior under flight, so how do they glean object range from image motion? The following paragraphs will cover some of the main points of insect navigation.

2.2 Stabilizing flight

A prerequisite for gleaning object range seems to be stable flight (Horridge, 1987; Srinivasan, 1993). In order to stabilize flight insects rely on there vision as there primary modality. Through studies W. Reichardt (1969) describes an optomotor response system, which controls stable flight. This system is capable of generating a range of counteractive movements (yaw, pitch & roll) if it's out of course. The studies by W. Reichardt also point to that perception of image movement is done by comparing image intensity variations in neighboring facets of the compound eye.

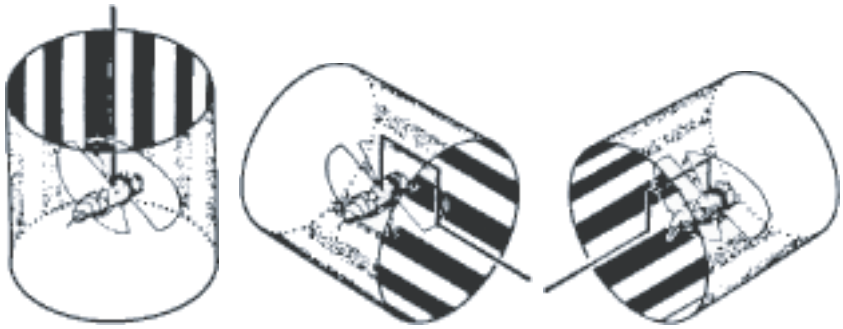

(a) Yaw (b) Pitch (c) Roll

Figure 2.1: The optomotor response

2.3 Controlling flight speed

It has been observed by C.T. David (1982) and Srinivasan (1996) that insects use the velocity of image motion over the eyes to control flight speed. In a series of experiments flies were taught to fly through a helical black and white stripped wind tunnel. The motion of the tunnel produced apparent image movement over the eyes, forwards and backwards. By adjusting the speed of the rotation of the tunnel, flies remained stationary in the air. They also seemed to have a fixed value, which the ground speed had to have. Thereby increasing and decreasing there speed to the fixed value. When the flies where exposed to a head wind they adjusted there trust as to maintain there fixed ground speed.

2.4 Distance flown

Recent studies from Srinivasan and Zhang (2003) point to, that bee's are remarkably good at relaying exact information about the position of e.g. a flower back to its fellow bee's. The way they do this is by doing a waggle dance which represents the distance flown; the longer the dance, the longer the distance. The distance which is relayed, is the optical flow experienced by the eye which is then integrated over time to estimate the distance flown. Further experiments by Srinivasan and Zhang where done, to see how external variables such as contrast and spatial frequency content of the environment, affect the distance measure. There results show that large differences in the contrast does not affect the amount of perceived optical flow information much, but stays at a near normal level. Even with different spatial frequencies the bee's distance and direction is not affected. Experiments

also show that the bee's centering response is unaffected when exposed to different spatial frequencies.

2.5 Negotiating narrow gaps

It is suggested by Kirchner and Srinivasan (1989) that bee's use the image movement over the eyes to center itself according to its surroundings and to fly through narrow gaps. This is done by balancing the movement on one eye with the movement on the other eye, thus trying to have the same amount of image movement on both eyes. Through a series of tests bee's where taught to fly through a grated narrow tunnel. Each side of the tunnel could be moved forward or backward in the horizontal plane. Figure 2.2A shows how the bee centers itself when the walls are stationary, but when one wall is moved in the same direction as the bee's flight [Figure 2.2B] it's trajectory shifted to the wall moving. When the wall was moved in the opposite direction the bee shifted towards the stationery wall. These findings demonstrate how the bee shifts its trajectory to the wall where there is reduced image movement according to the other eye. Kirchner and Srinivasan now wanted to be certain that it was only the image movement across the eye that was causing the shift and not that the bee was trying to balance contrast frequencies of the wall gratings. Figure 2.2D, E & F show how different spatial periods on one wall didn't have any affect on its trajectory.

Recent studies by Srinivasan and Zhang (1997) on the centering response showed that the centering response is direction-*insensitive* where as the optomotor response is direction-*sensitive*. In the initial experiments of the centering response the speed of the corridor walls never exceeded the speed of the insect, therefore not testing for direction sensitivity. Srinivasan and Zhang discovered this by rapid movement of the walls and later saw that they would get the same results for a wall moving upwards or downwards. This surprising result has led to the proposal of an independent visual pathway for the centering responds in flying insects which is direction-*insensitive*. The suggestion of this separate direction-*insensitive* pathway has also found anatomic evidence in flies (Douglass and Strausfeld, 1997).

M. Anthony Lewis and Mark E. Nelson have done similar findings for peering insects. They have shown that peering behavior also seem to be insensitive to the direction of motion. This actually leads us back to Exner (1891). His experiments with craps lead him to propose that they use the *rate of motion* to estimate depth.

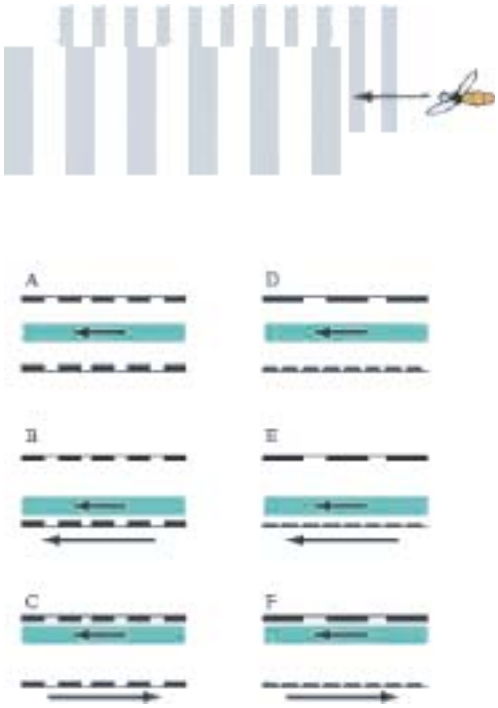

Figure 2.2: Negotiating narrow gaps

Further studies have shown that the image movement over the eyes isn't the only denominator. A correlation between the visual system and the optomotor response is used to move through the world. Certain instances of the image movement trigger an optomotor response while others trigger a self centering response.

Chapter 3

Motion Perception

We have seen that different experiments with flying insects, reveals their use of optical flow. Here we will take a closer look at the perception of depth, by means of motion detection. This investigation will lead us to a formal definition and explanation of optical flow. Finally we will describe and discus what we will call *Motion Energy*.

3.1 Depth perception

The world has four dimensions, three spatial and one temporal. All light-sensitive organs record light on a surface. This only leaves us with the capabilities to perceive two spatial dimensions directly. The third dimension of depth has to be reconstructed by the brain.

The human brain utilizes a variety of different cues too achieve the perception of depth [Figure 3.1]. Many of these have been known by painters since the renaissance. Some known cues are contrast, texture, geometrical perspective, size, and occlusion [1].

All of these cues are independent of motion and can be extracted from a static monocular image. Insects can not effort such a complexity in depth perception. As described earlier the fly brain has to conserve energy for other tasks. We saw that fly's with bigger brains were slower and less successful than its smaller brained counter part [2]. Optical flow presents such cost efficient solution to depth perception. Optical flow depends on detecting motion.

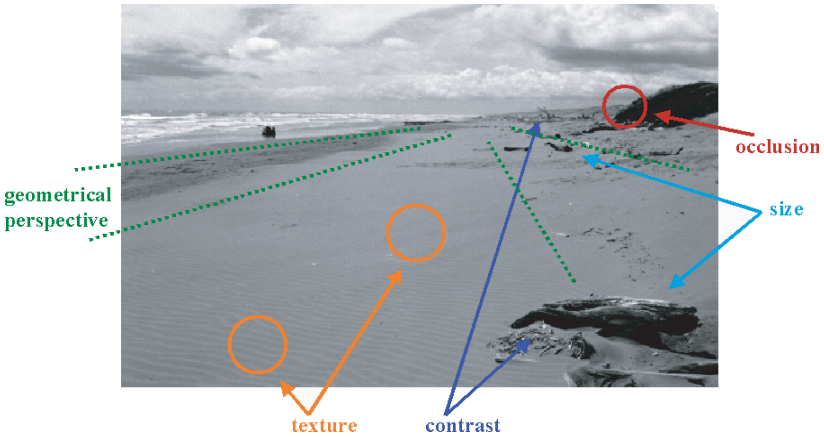

Figure 3.1: Pictorial cues

3.2 Motion in space

As we stated before, the world consists of space and time. Motion is the link between space and time. We need a perception of time to see motion. To perceive time we need some way to memorize two different instances of the present and determine a correlation between them. From this follows that time perception is an ability to divide time into intervals [3]. There has to exist a cross modality between light, and time sensory to perceive motion. This ability seems to be hardwired into the neurology of the eye. Such a construction can be denoted an EMD (elementary motion detector). Reichardt proposed a very simple EMD based on his fly studies, often referred to as the Reichardt detector [4]. It works by correlating two inputs, where the one is delayed. This delay realizes the need for time sensory; it gives the eye a memory. By adding multipliers, the model can also detect the direction of the motion [Figure 3.2]. Reichardt's model is one amongst a long line of different attempts to develop a functional model for fly vision.

3.3 Motion parallax

The fly's neurological construction can explain the ability to detect time, and thereby motion [Appendix A]. Motion detection opens a new door to depth perception. This relation between motions and depth perception was first discovered by Exner. He proposed what he named the *motion parallax*. It states that for a viewer in motion close objects will move faster over the field of vision than more distant objects [Figure 3.3].

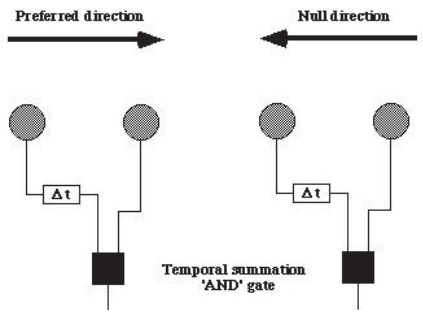

Figure 3.2: The Reichardt detector

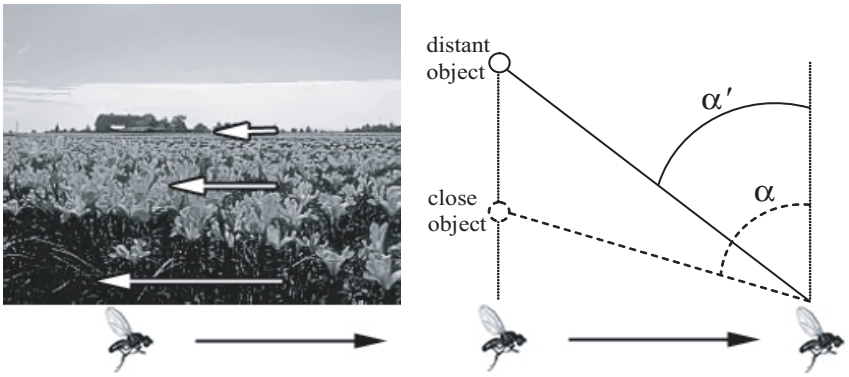

Figure 3.3: Motion parallax

A further investigation of this definition will reveal a relation between stereopsis and motion parallax. To do this we will look at three different cases, and try to evaluate them against each other.

- The first case is a fixed camera taking two images of the same scene with a time delay.
- The second case is a moving camera taking two images of the same scene with a time delay.
- The last case is two cameras at different positions each taking an image of the same scene with no time delay.

These three cases can be seen as different ways to determine the depth in the scene. In the first case we suffer from not having a reference to get

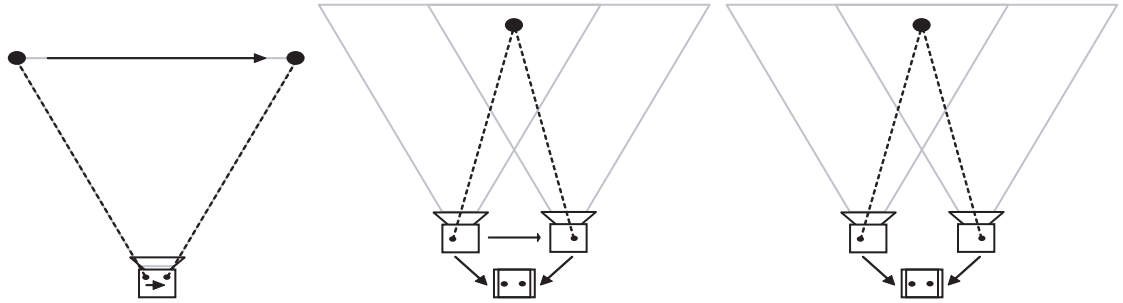

(a) Still camera with time delay (b) Still camera moving with time delay (c) Two cameras at different positions

Figure 3.4: Cases of motion parallax

precise measure. We depend on movement in the scene. We will only be able to state that fast moving objects are closer than slower moving objects. For no movement in the scene we will not be able to say anything about depth in the scene.

For the second case of the moving camera we will always be able to say something about the depth of the scene. As long as the scene is stationary we can determine the construction of the scene in terms of what is in front of what. Knowing the distance travelled and the time delay between the two images would give us a precise measure of a stationary scene. If the scene is not stationary, but consists of moving objects then follows; the faster we could move the set distance to take the next the image, the more precise our measurement would be.

This leads to the last case of stereopsis, where there is no time delay between the two positions from which the two images are taken, giving us perfect precision[1]. Stereopsis also gives the ability of stealth attack, for biological systems.

The common presumption for all cases is that differences between the two images are caused by changes in the scene. This however is only completely true for the last case of stereopsis where there is no time delay. In the two first cases we will have to consider a global illumination problem. This problem is in relation to the time delay, for a shorter time delay we have increasing precision. All cases represent the need for a precise spatial measurement of the displacement in the scene to derive depth. This problem has two elements first there is the measure of distance secondly there

[1]An interesting fact to review is the case where the set distance between the two images were to be travelled with a speed greater than that of light. That would, according to Einsteins speicial theory of relativity, add the fourth dimension of time.

is the correspondence problem which we will investigate later. For revealing distance information the last two cases presents the most obvious solution to the problem. If we consider the moving camera, it would need a separate way to measure its own distance travelled between the two images. In the case of stereopsis the displacement between the two eyes are constant, and an integrated configuration of the system.

3.4 Insect vision

A biological system not utilizing stereopsis needs a way to determine its own velocity. A resent study of peering behavior for depth perception has revealed some results that might explain how also flying insects cue distance. If the target of the peering insects distance gauging was moved the insects would miscalculate the distance. Furthermore it was only dependent of speed and not direction. These findings point to two important possible strategies for insect depth perception. Firstly it indicates that the insect presumes the target to be stationary. Secondly it's interesting that this behavior is also non-directional, as is the case with centering-response in flying insects. We could presume that in the evolution of flight in general goes from leaping to flying. The centering response visual pathway could then be an early adaptation from the peering leaping evolutionary stage that has been preserved to find other applications. This is supported by experiments on the flying insect's centering response. In our review of the centering response experiments we saw that they move away from a moving wall ignoring the direction of the movement. We could say that the insect perceives the wall to be closer. This is completely consistent with the presumption that the insect presumes the world to be stationary. The reason for this behavior could be seen in relation to experiments that have shown that honeybees will slow down as they approach narrow gaps.

This adjustment of speed according to the perceived angular speed over its eyes must then make use of separate sensory system. To determine speed independently of what it sees, also points on the assumption of a stationary world. Adding this modality enables the system to have the ability of measuring speed from the visual input.

As we now have shown three different sensory inputs are needed to use motion for depth perception in biological systems not utilizing stereopsis;

1 Sensory of light

2 Sensory of time

3 Sensory of speed

We have looked at differences and relations between different ways to use the connection between motion and the perception of depth. Flying insects such as fly's use loco-motion to estimate depth. This technique is called optical flow. In the following we will give a formal definition of optical flow and show how it can be derived. It was also shown that insects seem to have a non-directional sensitive visual pathway. We will look at how we can formalize this in a measure which we will call motion-energy.

3.5 From Optical flow to Motion Energy

Optical flow can be defined broadly as; the motion we perceive when we move though the world [5]. A definition related to digital video could sound as follows: A method for procedurally determining the movement of objects in an image examining the full sequence from which the image was extracted [6].

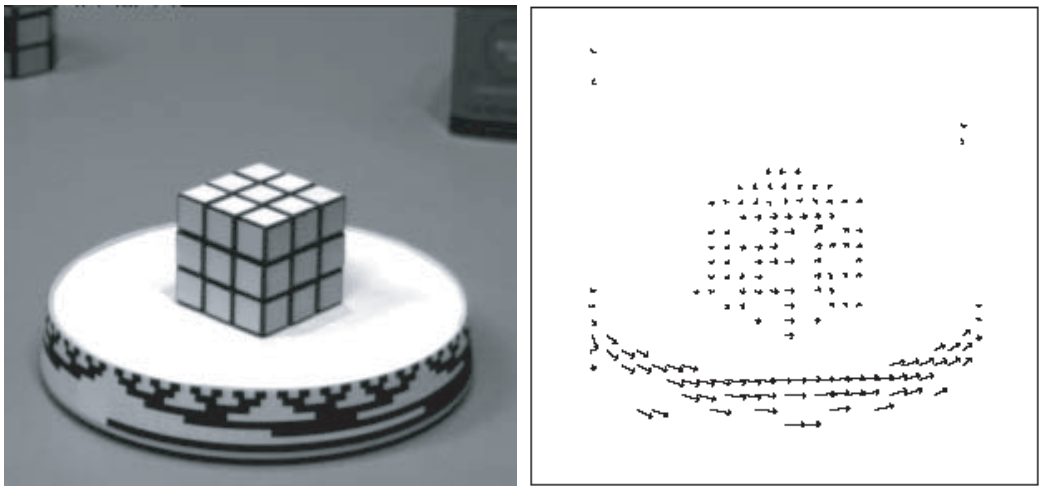

Figure 3.5: Flow fields for the Lucas and Kanade technique applied to real image data.

The basic assumption for optical flow calculations is that the brightness of an image does not change if there is no change in the image over time $I_t = 0$. We could say that a change in the images is caused by motion. By this assumption we can state;

$$\frac{dI\,(x, y, t)}{dt} = I_t \tag{3.1}$$

If we look at the intensity function $I(x, y, t)$ and assume that the change in the images is small, then the images are nearly alike. This leads to a function, where δx and δy are the displacement from $I(x, y, t)$ after the time δt:

$$I(x, y, t) = I(x + \delta x, y + \delta y, t + \delta t) \tag{3.2}$$

If we apply the Taylor series expansion to the flow we can get an approximation of the change of a point caused by motion. The e is the higher order derivatives:

$$I(x + \delta x, y + \delta y, t + \delta t) = I(x, y, t) + \delta x \frac{\partial I}{\partial x} + \delta y \frac{\partial I}{\partial y} + \delta t \frac{\partial I}{\partial t} + e \tag{3.3}$$

By subtracting $I(x, y, t)$ on both sides we get the equation also known as *brightness constancy constraint equation*(BCCE):

$$\frac{\partial I}{\partial x}\frac{dx}{dt} + \frac{\partial I}{\partial y}\frac{dy}{dt} + \frac{\partial I}{\partial t} = 0 \tag{3.4}$$

Another way to denote the constraint equation:

$$\nabla I \cdot \mathrm{v}^t + I_t = 0 \tag{3.5}$$

Where $\nabla I = (I_x, I_y)$ and I_t are the 1^{st} order partial derivatives of $I(x, y, t)$. ∇I is the spatial intensities gradient and the image velocity is $\mathrm{v} = (u,\ \nu)$. This can be simplified into the equation:

$$(I_x, I_y) \cdot (u, v)^T + I_t = 0 \tag{3.6}$$

$$I_x u + I_y v + I_t = 0 \tag{3.7}$$

The velocity vectors can be defined as;

$$u = \frac{dx}{dt}, v = \frac{dy}{dt} \tag{3.8}$$

This gives a representation of the optical flow.

One problem that arises is that we are only able to measure the component of the optical flow, where $\mathrm{v}_\perp$ to the gradient intensity. The tangential components to the intensity gradient can not be measured. This problem is also known as the aperture problem where different physical motions are indistinguishable. In [Figure 3.6] a line moving from left to right produce the same spatio-temporal structure as a line moving bottom to top.

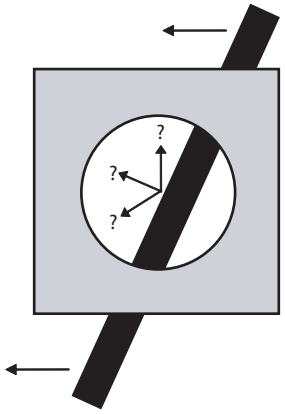

Figure 3.6: The aperture problem

3.6 The correspondence problem

So far we have ignored the problem of determining correspondences between images over time. As the definition we have given above holds for all optical flow computations techniques, they mostly differ in there approach to correspondence. Correspondence falls in two main groups; appearance and feature-based methods. The appearance-based technique measures the correlation pixelwise between two images. Feature-based techniques will look for the most identifiable parts of an image and find a match in the next image. For insect vision most suggests appearance-based methods for finding correspondence. Flies are believed to use some system of auto-correlation as we saw in the Reichardt detector where a signal is correlated with a delayed version of itself. We will not go into a deeper investigation of different techniques for a detailed review. Instead we will propose a model for calculating non-directional optical flow.

3.7 Motion Energy

The model for calculating non-directional optical flow we have denoted motion energy. Achieving a centering responds is a special case, which allows for certain simplifications based on some assumption that can be stated in this case. In the description of the different experiments with flying insects we saw that flies seem to have a separate visual pathway responsible for the centering responds. We saw that the fly ignores the direction of motion in its field of vision. The fly will center itself in a corridor in correspondence to the

angular speed of visual inputs over its eyes. If this is true we can state that the omni directional optical flow in this special case can be directly defined as the change in light intensity over time. We will denote this motion energy with E. The motion energy is calculated by first normalizing the image values, where after a temporal interval of 2 is added. To stabilize the values we lastly sum the mean of difference of the motion energy in the left and right side over 20 samples. Motion energy can now be denoted;

$$E = \int \left| \frac{\partial}{\partial t} I\left(x\right) \right| dx \tag{3.9}$$

$$E = \int \left| I_t\left(x\right) \right| dx \tag{3.10}$$

3.8 The contrast problem

This definition will leave us with the problem of this motion energy being dependent on contrast. A high contrast will yield high motion energy and vice versa [Figure 3.7].

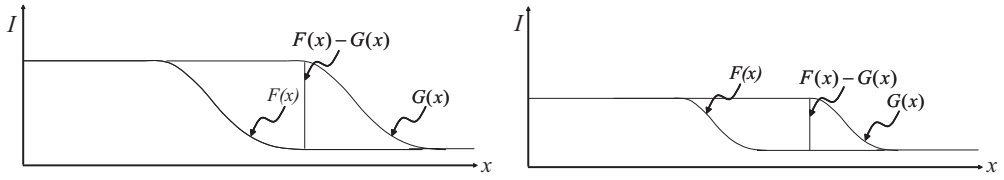

(a) HIGH contrast (b) LOW contrast

Figure 3.7: Shows that $F(x) - G(x)$ depends on contrast

For an 8 bit gray scale image the calculation will be;

$$I = \frac{I - I_{min}}{I_{max} - I_{min}} \cdot 255 \tag{3.11}$$

We have now insured that each eye has a maximum contrast, independently of the global contrast of the input. (See figure 4). This leaves us with another problem of the possibility of having a non uniform amount of contrast peaks and valleys. This is bad since more peaks and valleys will mean more motion energy. By smoothing the image prior to the contrast maximization, we insure that only one peak and valley per eye exists.
Since the size of each eye is 10 x 10 pixels, a 5 x 5 smoothing kernel has been applied to the input image before the extraction of the eyes [Chapter 4, Figure 4.4b].

(a) Not smoothed, original contrast

(b) Not smoothed, maximum contrast

(c) Smoothed,original contrast

(d) Smoothed,maximum contrast

Figure 3.8: The contrast problem

3.9 Noise

As we now have a uniform output from each eye we can calculate the motion energy by computing the absolute difference over time for each eye [Equation 3.12]. This result will however suffer from background noise. Let's return to the statement that for no motion there will be no change in brightness intensity over time as assumed by the *BCCE*;

$$I\left(\vec{x}\cdot\Delta\vec{x}\right)=I\left(\vec{x}\right),\quad \vec{x}=(x,y,t) \tag{3.12}$$

This is not the real case. In reality we have to deal with background noise and illumination changes. The illumination effect can be reduced by reducing the time interval. The background noise can be dealt with in different ways. We have chosen to high pass our motion energy result. This is coherent with the biological evidence of the visual system of the fly. It seems to ignore small motion [Chapter 4].

3.10 Determining the motion energy field

To achieve a centering respond two different approaches can be considered. Either to move towards less motion energy or to move away form most motion energy. We have chosen the latter approach. This is due to the fact that the high passed motion energy readings in some cases will be zero in more than one eye. To decide which zero reading to weight highest can become a problem. Such an algorithm to find the best direction would anyway have to take all eyes in to consideration. This being the case, avoiding most motion reveals a simpler solution and has therefore been our choice. To determine the difference of motion energy between the left and right side, we will only

consider eyes looking to the sides. This will be the eyes in the range from 0 to 45 degrees and then the eyes from 135° to 180°.

The result will then be handled by our control loop which is similar to the control loop of the first experiment.

```
for(int i=0; i<number_Of_Runs; i++)
{
    send_Command("move 20 cm");

    if(Math.abs(opticalFlowDiff) > 10)
    {
        if(opticalFlowDiff >0)
        send_Command("rotate -10 d");
        else
        send_Command("rotate  10 d");
    }
}
```

Figure 3.9: The Control Loop

Chapter 4

Experiments

The motion energy solution described earlier is based on knowledge gained through research of the visual system of the fly. This research has also given us an understanding of the biological structure of the fly eye.
The motion energy solution is implemented into a robot, where the motion energy will be utilized to create a centering responsive behavior. Through a series of test runs the robots performance will be observed and registered.

4.1 The biological structure of the compound eye

The structure of the compound eye is divided into several layers (*lamina, medulla and the lobular complex*), where the processing of the visual input is done for creating an output to the motor system of the fly. These different processing layers will not be covered, due to the complexity and diverse conclusions within the research. For a more detailed biological description see [Appendix A]. Instead a description of the basis of the visual system of the eye will be introduced.

The visual organ of the fly is called the *compound eye* [Figure 4.1a], which consists of facets or ommatidia. Compound eyes, depending on species vary from 700 facets in the fly to over 25,000 in dragonflies. The light entering the cornea of a single ommatidia is sampled from one direction in the visual field. As light passes down the ommatidia, light sensitive cells are stimulated and nerve impulses are fired off to the brain. The ommatidia are spread over the compound eye and thereby covering most of the surface of a hemisphere [Figure 4.1b, 4.1c]. Flies have fixed a lens which makes their spatial resolution bad, but to compensate for this they have a high temporal resolution.

The high temporal resolution makes it excellent in detecting motion in the visual field.

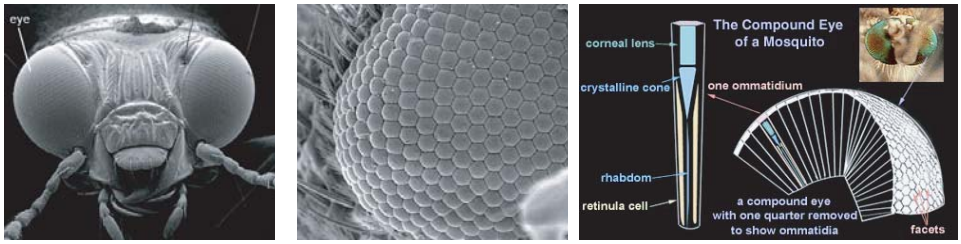

(a) The fly head (b) The compound eye (c) The ommatidia

Figure 4.1: The fly eye

4.2 Motion Energy experiment

To restate the problem that we wish to solve; The goal for our experiments is to test centering responsive navigation based on our motion energy solution as described in chapter 3.

4.2.1 Test environment

The environment [Figure 4.2] where the test runs are performed is constraint to a corridor. It's important that the corridor is quite uniform and the floor is level, otherwise it could disturb the results of the experiment. The size of the corridor is h 263 cm x w 223 cm x d 2500 cm.

Figure 4.2: The environment

4.2.2 Evolution Robotics ER1

The hardware for testing the experiments on is the ER1 personal robot system from Evolution Robotics. Interfacing the ER1 is done through a command line API, which gives the ability to develop advanced behaviors and algorithms to control the ER1.
The ER1 comes pre-assembled and is delivered in several pieces. This gives a freedom of creating custom built robots that meet the specifications of ones needs.
Since the brain of the robot is a laptop; here are some minimum system requirements:

- Pentium III class, Intel Celeron , or AMD processor - 500 MHz or faster
- 128 MB RAM
- 250 MB Hard Drive Space
- Two USB ports (one for the camera and the other for connecting the robot to the laptop)
- Laptop monitor must be able to support a 1024 x 768 screen setting
- Microsoft Windows 98, Windows Me, Windows 2000, or Windows XP

Here are some specifications of the ER1:

- approx. size: 60cm x 30cm x 40cm (H x W x D)
- approx. weight: 10kg without the laptop
- max. velocity: 50 cm/sec = 1.8 km/h
- max. angular velocity: 90 degrees/sec

The system which the experiments are going to be conducted on has the following specifications:

- Intel Pentium M class, - 1400Mhz
- 512 MB RAM
- Supports a 1024 x 768 screen setting
- Microsoft Windows XP

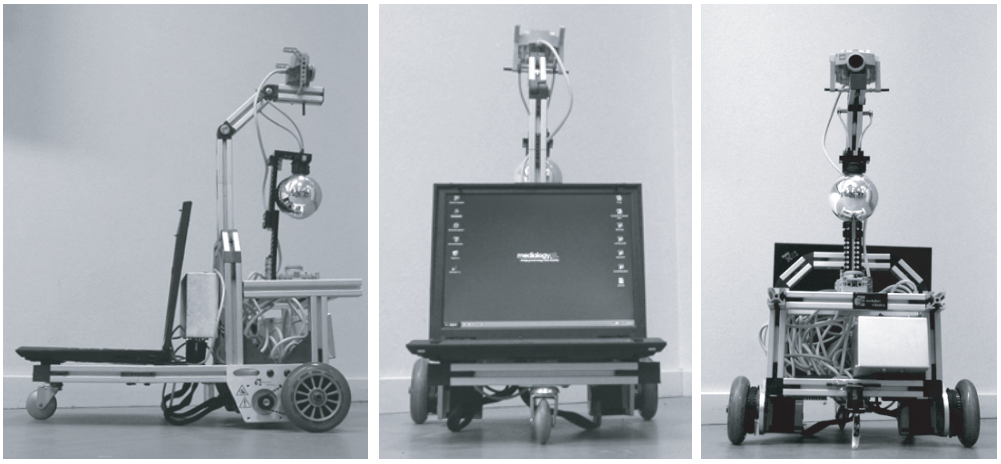

(a) Side View (b) Back View (c) Front View

Figure 4.3: The ER1 Robot

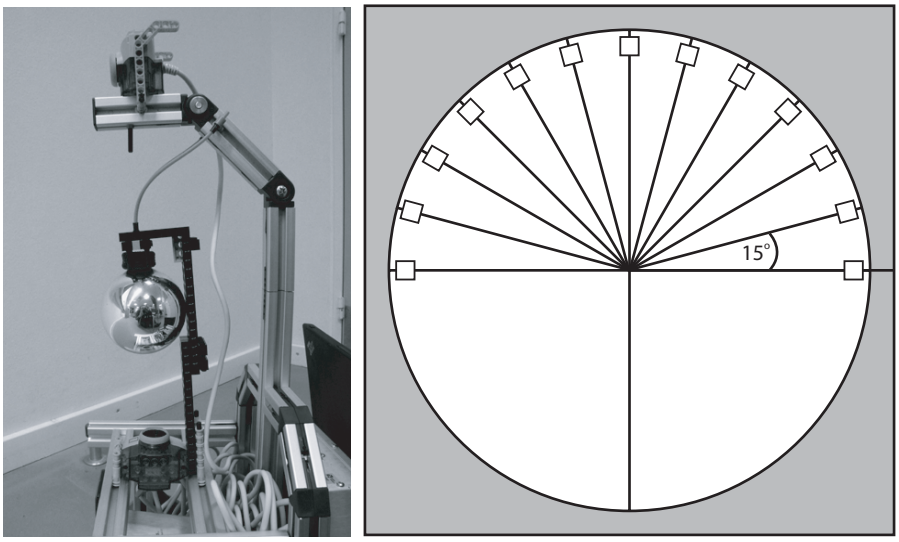

(a) The spherical camera setup (b) Our eye setup

Figure 4.4: The ER1 Robot camera setup

The Visual System

Looking at the fly's compound eye, we see a surface of facets which covers most of the hemisphere. Inspired by this we derived to a solution which

incorporates a reflective sphere placed over a camera [Figure 4.4a]. This gives us a panoramic view of the world. The compound eye consists of hundreds to thousands of facets. Due to this complexity, it became a matter of analyzing our problem and creating a solution which was satisfactory in order for us to achieve our goal. The first thing that became evident with the panoramic view was the indifference in the visual field behind the robot. Therefore the interest lied in the frontal 180°, because the robots goal was to drive down a corridor. Inspired by the compound eye and its facets; we created 13 patches, which were extracted along the horizon of the frontal 180° panoramic view [Figure 4.4b]. The size of each patch was 10x10 pixels and separated by 15 degrees, hereby covering 180° in total.

4.2.3 Results

The results are based on two tests, due to hardware problems, which will be discussed in section 4.3. Despite this they provide a clear picture of strengths and weaknesses of the Motion Energy solution. They provide crucial information on things that can be improved or applied.

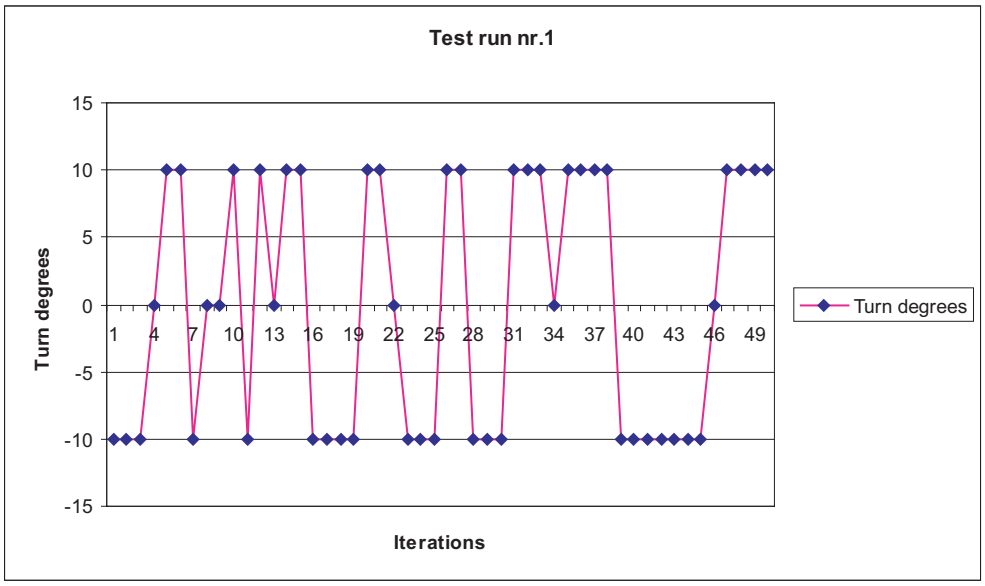

Figure 4.5: Test run nr.1; Turn degrees of ER1 over 50 iterations using motion energy

A test utilizing the Lucas-Kanade-Tomasi (LKT) feature tracker can be found in [Appendix B]. This test has been performed for comparative reasons.

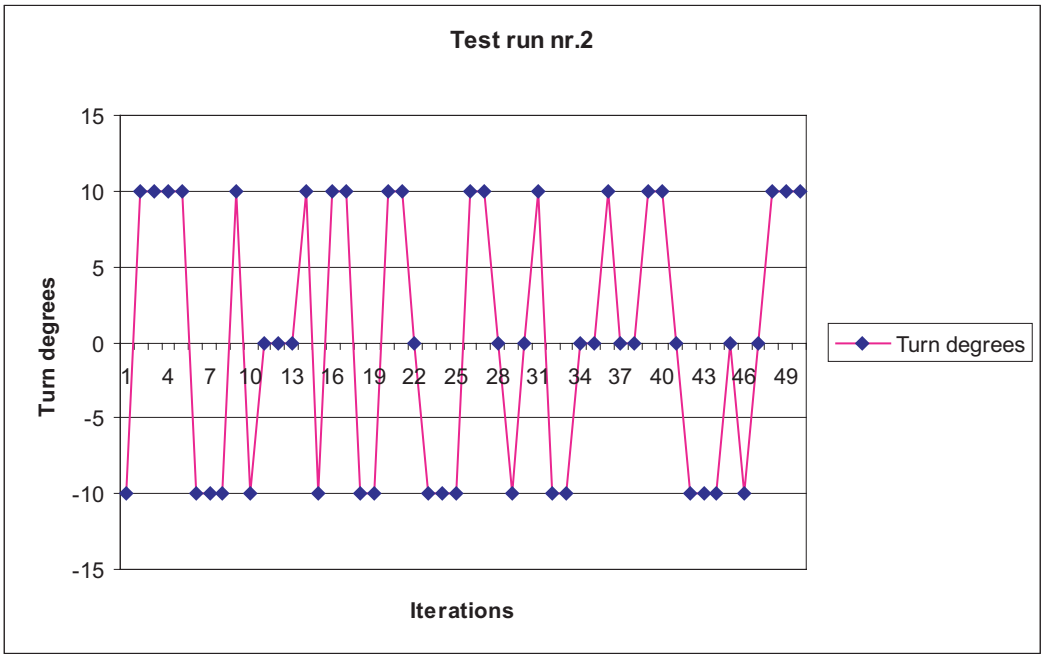

Figure 4.6: Test run nr.2; Turn degrees of ER1 over 50 iterations using motion energy

What becomes evident when looking at the two runs is the similarity of the oscillation down the corridor, caused by turns which are triggered by the Motion Energy flow difference [Figure 4.5]. The high oscillation actually fits well with the theory of the fly being short sighted. This is in conjunction with, that the robot needs to be close to the wall in order to make a decision to turn. It also illustrates, that the centering response can not be seen directly when observing the robot. The centering response is "visible" when considering the motion energy weighting between the left and right side of the robot. A possible solution for this is discussed in section 1.4.

The similarity between test run nr.1 and nr.2 seem to show, that some common features down the corridor are detected by the robot. In our case the obvious objects would be the doors and the lockers in corridor. The noticeable difference can be a result of the global illumination problem, but more likely due to the motion energy flow difference between the two test runs [Figure 4.6][Figure 4.7].

Furthermore [Figure 4.7] shows some high fluctuations. The highest fluctuations seem to occur when the robot is attacking the wall at an approximately 45 degrees angel and is very close to the wall. At this angel the

difference between the left and right side of the robot to a wall surface is greatest. This will be discussed in section 4.3.

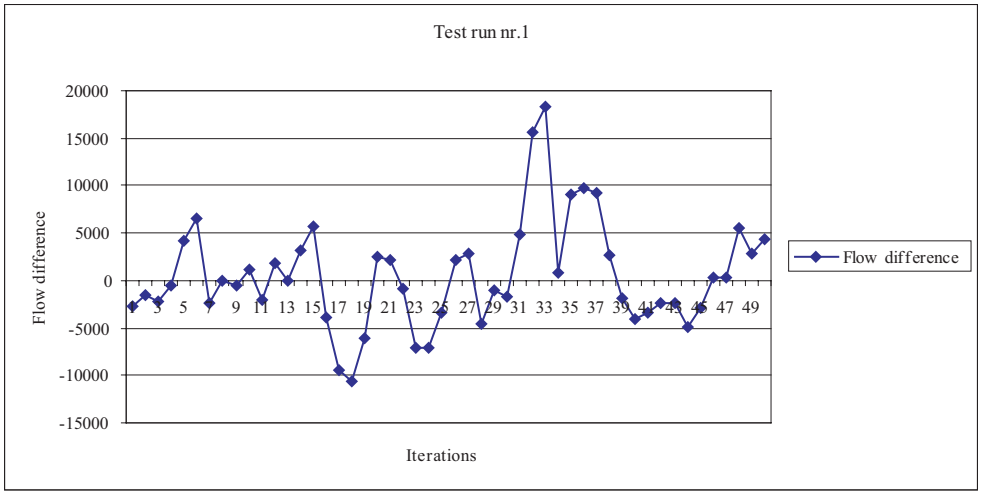

Figure 4.7: Flow difference of Test run nr.1 over 50 iterations using motion energy

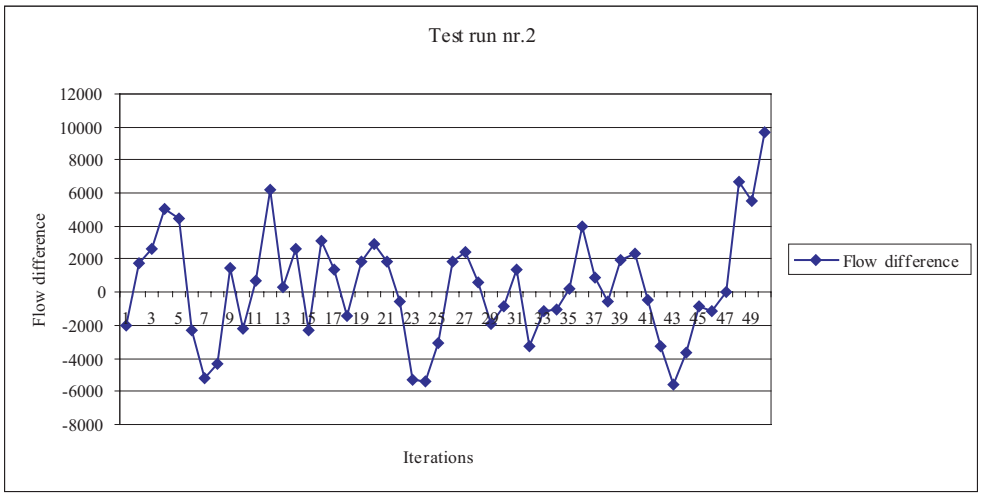

Figure 4.8: Flow difference of Test run nr.2 over 50 iterations using motion energy

Another experiment was performed, where the Lucas-Kanade-Tomasi feature tracker was used with the spherical camera[Appendix B]. The obvious

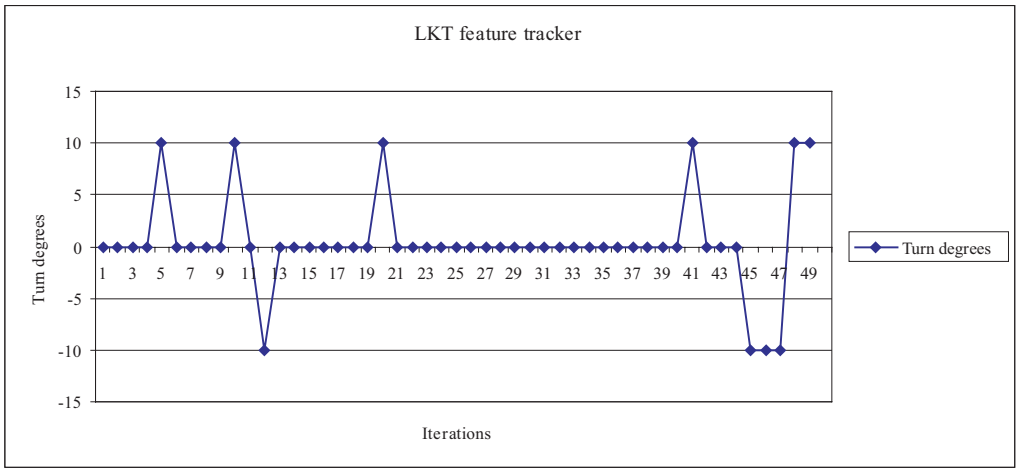

Figure 4.9: Test run og LKT

difference between the LKT and our Motion Energy solution was that the LKT performed at better centering responsive behavior [Figure 4.8]. The result is due to that the LKT is based on tracking features within the image plane over time. Its weakness however is a combination of contrast and illumination problems. It can not detect motion if there are no contrast differences in the image plane, but also a misleading tracking caused by the illumination problem occurs.

The strength with detecting motion energy is that computational wise it's lighter than for example the LKT. This is due to that it only detects motion on each side of the robot and compares them to each other. Our solution ignores correspondence. Unlike the LKT which has to track pixelwise in order to detect motion, this requires more computation.

4.3 Discussion of results

One of the key observations during the test runs was the high oscillation when the robot navigated down the corridor. The reason for this behavior is that the robot assumes a direct similitude between the motion energy in a certain eye and the distance to an object. This assumption does not take the perspective as seen through the sphere into account. If we consider the robot rotating around is own axis close to a wall, the difference between the measured and the actual distance increases with the angle to the wall. A possible solution could be to delay the view of which the motion energy

calculation is done from. Let's examine the approach in respect to the setup of our robot. Each eye is separated by 15 degrees. If the robot makes a turn we could assume that it to be a turn away from the wall. Then we shift the view of the robot by one eye (15 degrees) in the opposite direction of the turn. Another solution would be to weight the different eyes influence on the sum of motion energy on each side in respect to the amount of motion energy in the individual eyes. Higher motion energy gets higher weighting. This weighting could be based on the assumption that the eye with highest reading is said to be perpendicular to the wall. As we also know the separation of the eyes to 15 degrees, we can set the weighting as follows;

$$E = \frac{E_{max}}{\tan |E_{max}\theta - E\theta|} \tag{4.1}$$

Our experiments are also limited by the hardware used. The ER1 lacks the ability to turn and drive at the same time, which makes it impossible to get "realtime" feedback. If it had this ability, it would allow us to implement the weighted influence on each eye, to determine the velocity and turn angle of the robot.

Chapter 5

Conclusion

Inspired by the visual system of the fly we have derived to a solution, which utilizes the basic theories and research behind this system. Choosing this insect was due to its biological simplicity and processing to visual stimuli. However through research has led us to the conclusion, that the visual system of the fly is far more complex than first anticipated. This is why basic and well documented theories have been the main source of inspiration to our solution.

Through experiments with motion energy we have created a robot, which is centering responsive in its navigation down a corridor. With the motion energy solution applied to the robot it performed well, but also as expected in correspondence to the research of the visual system of the fly. This was proved by the oscillating behavior due to the motion energy flow differences between the left and right side of the robot.
Comparing the motion energy solution to the LKT feature tracker shows, that motion energy is less sensitive to illumination variances, as seen with LKT.
An interesting aspect of our motion energy solution was its simplicity compared to its performance in perspective to other robot navigation solutions. It gives food for thought when developing biological inspired solutions. This is especially evident in our creation of the camera setup.

Under the process of developing this project a dispute occurred, due to the project formalization demanded a merging of senses. Merging of senses interprets as one or more senses. Our solution only utilizes one and the reason for this is based on performance. The experiments proved that the robot centering responses performed well by only utilizing the visual sense. Therefore a decision was made not to incorporate other senses (audio, IR), because

it wouldn't improve the performance of the robot compared with project goal.

Future Work

Looking ahead there are several improvements that could be implemented to enhance the robot. These improvements could be utilizing more senses, even though it wasn't found necessary in this project in order for us to achieve our goal. A sense which would be particularly interesting would be the sense of equilibrium. This would be an advantage e.g. if the robot operated outdoors, where rocky terrain and other forces of nature would come into play against the detection of motion energy. Other sensors could also be applied, which could back-up the primary sense; in our case the camera vision and thereby enhance the chance of the robot being "tricked".
Improvements on the detection of motion energy could also be improved. For example using more patches for comparing the motion within the vision system.

Bibliography

[1] http://www.pc.rhul.ac.uk/zanker/teach/PS1061/L4/PS1061_4.htm*(last viewed 11-02-05)*

[2] http://nootropics.com/misc/smartflies.html*(last viewed 11-02-05)*

[3] http://plato.stanford.edu/entries/time-experience/*(last viewed 11-02-05)*

[4] Christof Koch,"Models of Motion Perception: Introduction and The Reichardt Correlation Model," *California Institute of Technology, Koch Laboratory, Pasadena, USA*, January 2004

[5] http://www.centeye.com/pages/techres/opticflow.html*(last viewed 11-02-05)*

[6] http://www.highend3d.com/bookstore/?section=compositing#0121339602*(last viewed 11-02-05)*

[7] Fabrizio Gabbiani,"How neurons interact together,"*Integrative Neuroscience*, Lecture 27/28, 2004

[8] Mert Sarikaya, Wenxia Wang and Haluk Öğmen,"Neural network model of on-off units in the fly visual system: simulations of dynamic behavior,"*Department of Electrical and Computer Engineering, University of Houston*, Houston, Texas, USA

[9] http://www.fortunecity.com/greenfield/buzzard/387/, Basic Neurology Made Easy

[10] Ann B. McNaught and Robin Callander, "Illustrated Physiology," *Edinburg*, 1970

[11] Martinus Jansen, "Information processing by spiking neurons in the first optic chiasm of the blowfly," *University of Groningen*, Netherlands, chapter 1, 1998

[12] Jianbo Shi and Carlo Tomasi, "Good features to track," *IEEE Conference on Computer Vision and Pattern Recognition*, Seattle, 1994

[13] Mandyam V. Srinivasan and Shao-Wu Zhang, "Visual navigation in flying insects," *Center for Visual Science, Research School of Biological Sciences, Australian National University, Canberra, Australia*

[14] Susanne A. Huber, Matthias O. Franz and Heinrich H. Bülthoff, "On robots and flies: Modeling the visual orientation behavior of flies," *Max Planck Institute für Biological Cybernetics*, Tübingen, Germany

[15] Susanne A. Huber* and Heinrich H. Bülthoff*, "Visuomotor control in flies and behavior-based agents," **Friedrich Miescher Laboratory of the Max Planck Society*, Tübingen, Germany, ***Max Planck Institute for Biological Cybernetics*, Tübingen, Germany

[16] Adrian Horridge, "Pattern and 3D Vision of Insects," in Yiannis Aloimonos (Eds.), *Visual Navigation - From Biological Systems to Unmanned Ground Vehicles*, University of Maryland at College Park, 1997

[17] Bruce D. Lucas and Takeo Kanade, "An Iterative Image Registration Technique with an Application to Stereo Vision," *Proc. DARPA IU Workshop*, pp. 121-130, 1981

[18] S.S. Beauchemin and J.L. Barron, "The Computation of Optical Flow," *Dept. of Computer Science, University of Western Ontario, Canada*, pp. 5-9, 1995

[19] Christof Koch, "Models of Motion Perception: Introduction and The Reichardt Correlation Model," *California Institute of Technology, Koch Laboratory, Pasadena, USA*, January 2004

[20] Evolution Robotics, "ER1 User Guide version 1.0.2," Pasadena, California, USA, 2002

[21] http://flybrain.neurobio.arizona.edu/

[22] http://en.wikipedia.org/wiki/Action_potentials

Appendix A

The visual system of the fly

A.1 The Compound Eye

In order for us to find visual navigation based on inspiration from the biology of the visual system of a fly, it's important to get an understanding of the structure and function of the fly eye. This knowledge can have a direct influence on the solutions and even more help to evolve other ideas.

A.1.1 Ommatidia

The fly eyes are called *compound eyes*, which consists of facets or *ommatidia*. Compound eyes, depending on species vary from 700 ommatidia in drosophila to over 25,000 in dragonflies. The light entering the cornea is sampled from one direction in the visual field.
Hereafter a crystalline cone focuses the light down the central axis of the rhabdome. In the rhabdome 8 photoreceptors (R1-R8), through chemicals similar to humans transform the light energy to electric energy.
Around the 8 photoreceptors, pigment cells separate one ommatidia from its neighbors. Depending on what kind of insect, the photoreceptors can absorb different wavelengths of the incoming. This makes it able to distinguish between different colors, e.g. bees use colors and ultraviolet to find flowers. Each photoreceptor sends an axon down to the lamina for further processing of the signals from R1-R6.
R1-R6 are sensitive to low intensity light and small wavelengths, whereas R7 and R8 are sensitive to high intensity and large wavelengths, but with respect of the pigment cells [7].

The resolution of the compound eye is determined by two things. First the number of ommatidia, but secondly by the angle between two ommatidia.

The angle between two ommatidia is $\Delta\varphi$, where $\Delta\varphi$ is the ratio between the diameter of a single facet to the radius of the eye [7].

One of the strengths of the compound eye is it's excellence in detecting motion. This due to the *flicker rate* in compound eyes is ten times faster than a human eye. Humans see an image 30 times per second, while flies flicker rate reaches 300 times per second. This means that flies have a poor spatial resolution, but an excellent temporal resolution. The temporal resolution helps it detect the slightest motion in the visual field.

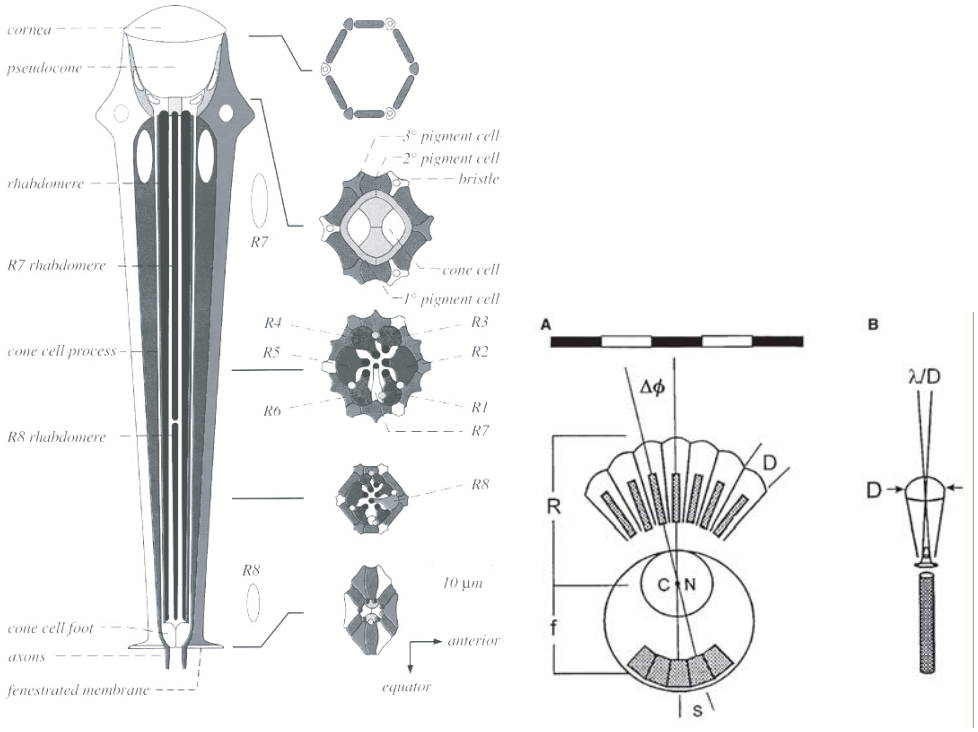

(a) Ommatidia

(b) Resolution determination of the Compound Eye

Figure A.1: The Fly Eye

A.1.2 Lamina

In the lamina the axons from R1-R6 are superposed onto LMCs (large monopolar cells) in the same cartridge. The axons from R7 and R8 bypass the lamina and send there axons directly to the medulla.

The signal from ommatidia is processed in the lamina by 3 LMCs (L1-L3), the amacrine cell (AM), 2 monopolar cells (L4 and L5) and a basket cell (T1).

The 3 LMCs L1-L3 which are directly connected to the photoreceptors produce a transient hyperpolarized graded potential signal to light stimulus [8]. This means, when a photoreceptor is stimulated by light; the LMCs neuron membranes change electrical potential when the stimulation occurs. This is due to the graded potential which is responsible for firing an action potential, in that the greater the light stimulus the more channels of ions are open and thereby the change in voltage is increased. Due to that the graded potential controls the "gates" of when the action potential triggers, it can be seen as the threshold of the action potential.
The action potential is triggered, because of the concentration difference of K+ and Na+ inside the neuron compared to the outside of the cell. The potential fires when the concentration difference reaches a certain threshold. When the threshold is reached, the action potential self propagates.
The neuron is activated by stimulation; causing Na+ from outside the cell

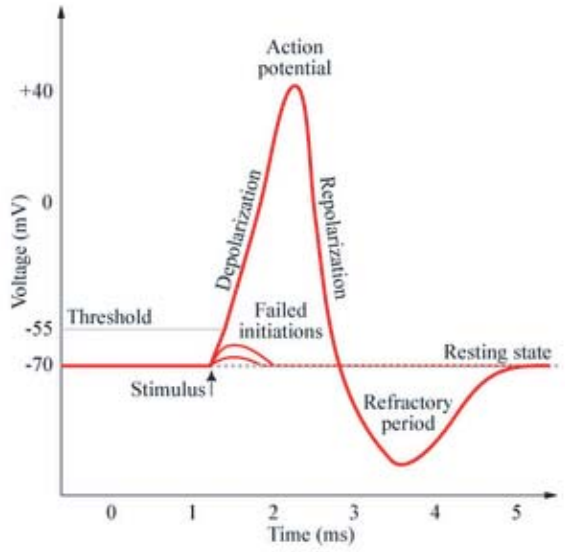

Figure A.2: Action Potential

membrane to flow into the cell. This causes the membrane to *depolarize* and trigger the action potential, because the inflow of Na+ changes the outside polarity from positive to negative.
The action potential releases neurotransmitters, which send signals to other neurons. Within a timeframe K+ flows out the cell and thereby *repolarizes*

the cell membrane. This timeframe is also called the *refractory period*. Doing the refractory period the neuron can not react on new stimulations until it reaches its resting potential.
The *hyperpolarization* functions as an inhibitory response to the graded potential and thereby making it harder for an action potential to occur [9][10].

Little is known about the amacrine and the T1 basket cells. It's suggested that the basket cell produces graded hyperpolarizations like the monopolar cells L1-L3 and knowledge on the amacrine cell consists of their anatomical characteristics .

Arnett DW discovered spiking units within the lamina, which are said to correspond to the monopolar cells L4 and L5. The spiking units can be divided into two groups. One group responds to the negative and positive change in light intensities, thereby increasing the spiking activity. This group is also called on-off units. The other group is called sustaining units. There spike activity is constant to a constant light intensity.
Due to the mere fact that on-off and sustaining units are said to correspond to the monopolar cells L4 and L5, a lot of researchers are conducting experiments within these cells to prove Arnett DW's findings [11].

A.1.3 Medulla and Lobular Complex

The medulla is not very well investigated, because it's been difficult to maintain stable recordings of the neuron activity. This is partially due to its small size. Even though, it's suggested that the sensation of motion is perceived here, because motion sensitive cells are not found in the lamina, but also because the lobular plate is known to receive inputs on motion sensitivity [7].

The lobular complex consists of the lobular and the lobular plate. Large neurons within the lobular plate detect wide-field motion both horizontally and vertically. These horizontal and vertical systems contain tangential cells, which have dendrites that span out through the lobular plate. The dendrites receive inputs from other neurons. Due to there connection to the tangential cells and there reception of inputs, they are able to process motion across the visual plane.
This processed motion within the lobular complex is connected to the optomotor system. The motor system controls the flies' orientation, heading and speed with a consideration to surrounding environment.

Appendix B

The LKT experiment

B.1 Experiment 1

A live input from a webcam is divided into a left and right eye. By evaluating the optical flow of the two eyes, the robot will rotate its self towards the lowest optical flow recordings.
If the absolute differences between the optical flows in the two eyes are below a set threshold the robot will continue without rotating.

B.1.1 Where to look

The size of the two extracted sub images to represent the left and right eye is chosen to make it big enough to display recognizable features, and small enough to allow for fast computation. Since the robot only moves in the plane of the floor, the two eyes are horizontally centered [figure B.1].
For the same reason we will only calculate the x component of the optical flow. By ignoring the y component we also reduce noise produced by tracking errors along the y axis [figurefig:t1t2].

If we consider a door panel moving through the scene, the lack of vertical features may cause the tracking to fluctuate horizontally [figure B.3].

For the optical flow calculations in the two eyes we are using the Lucas Kanade feature tracking.

The LKT Tracker

This tracker also called LKT (Lucas, Kanade & Tomasi) has been introduced by Shi and Tomasi [12]. This algorithm is based on finding the best feature to track. It stores the features and list them after how good they are to track. It is a selection based on dissimilarity. A corner that has high contrasts in both

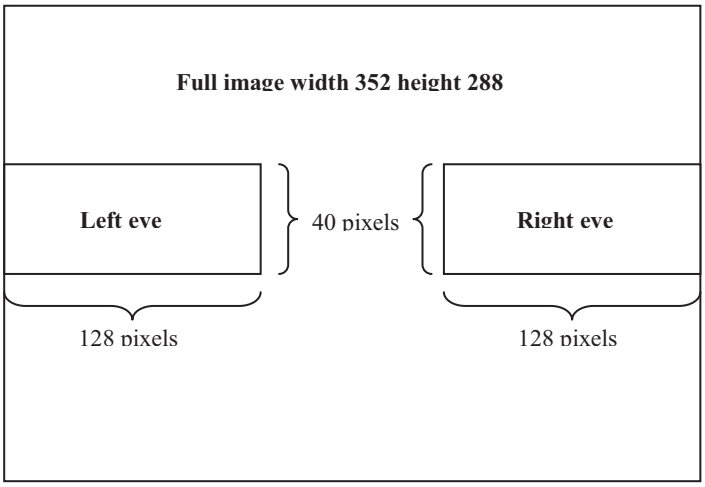

Figure B.1: Image display size.

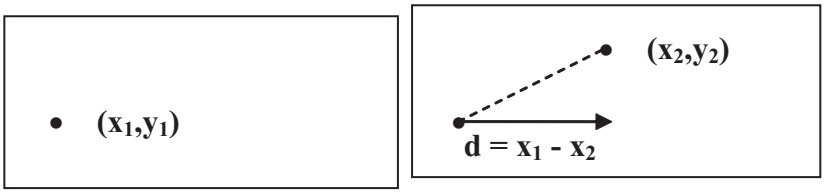

(a) Tracked point at T_1 (b) Tracked point at T_2

Figure B.2: Calculating the movement

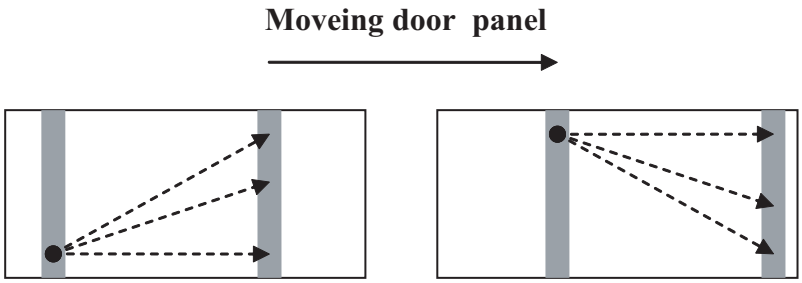

Figure B.3: A door panel moving across the scene.

x and y direction will be a good feature. A variable is set to the minimum distance between tracked points, to insure a spread in the tracked points. As a point is lost a new point is selected automatically. The eigenvalue of a matrix equivalent to good features will be evaluated to find best tracking candidate.

B.1.2 The Control Loop

The first task of the control loop is to evaluate the absolute value of the optical flow difference against a set threshold. If the value is under the threshold the agent will continue forward for 20 cm.
If the value is above the threshold it is evaluate to be greater than zero, if so the agent is commanded to rotate ten positive degrees, else the agent is commanded to rotate ten negative degrees.[figure B.4] The control loop is

```
for(int i=0; i<number_Of_Runs; i++)
{
    send_Command("move 20 cm");

    if(Math.abs(opticalFlowDiff) > 10)
    {
        if(opticalFlowDiff >0)
        send_Command("rotate -10 d");
        else
        send_Command("rotate  10 d");
    }
}
```

Figure B.4: The Control Loop

designed to be robust and as simple as economic as possible. By limiting the agent to a ten degrees rotation we saturate the forward motion, stabilizing the optical flow difference. For a task more complicated than corridor centering an elaboration of the loop would be necessary. However this basic and restricted approach is a design to fit the task of corridor centering.

B.1.3 Results

The results from the first two tests showed that the robot had a tendency to drive towards a white wall on one side of the corridor. The reason for this was that the LKT tracker, tracks features and a white wall has none. To overcome this problem and to get some useful results the wall was covered with a cardboard plate with writing on.
The results from the new test [figure B.5] environment showed that it has a good centering responds. Looking at [fig1] iteration 21-41 it can be seen that it balances the optical flow evenly between both eyes. The spikes represent each time it turned and therefore the big difference in flow. The high peaks are due to the rotation of the robot. Except from the problems of tracking the white wall the agent was able to perform the task of avoiding collision with walls and steer down the corridor.

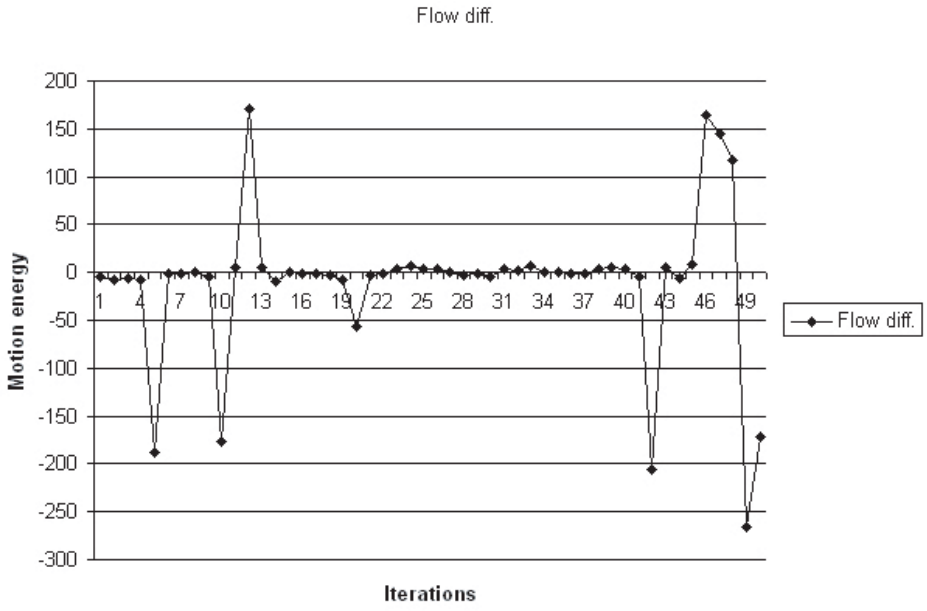

Figure B.5: Test

Appendix C

RAW data sheets

LK Test 1 -10d covered walls runs30

Run nr1 0 deggres flowDiff was: -7
Run nr2 0 deggres flowDiff was: -3
Run nr3 0 deggres flowDiff was: -2
Run nr4 0 deggres flowDiff was: -10
Run nr5 +10 deggres flowDiff was: -155
Run nr6 0 deggres flowDiff was: -6
Run nr7 0 deggres flowDiff was: -3
Run nr8 0 deggres flowDiff was: -6
Run nr9 0 deggres flowDiff was: 1
Run nr10 +10 deggres flowDiff was: -145
Run nr11 0 deggres flowDiff was: -3
Run nr12 0 deggres flowDiff was: 8
Run nr13 0 deggres flowDiff was: 10
Run nr14 0 deggres flowDiff was: 7
Run nr15 0 deggres flowDiff was: 1
Run nr16 -10 deggres flowDiff was: 191
Run nr17 0 deggres flowDiff was: 3
Run nr18 0 deggres flowDiff was: -1
Run nr19 +10 deggres flowDiff was: -98
Run nr20 -10 deggres flowDiff was: 122
Run nr21 0 deggres flowDiff was: -8
Run nr22 0 deggres flowDiff was: -6
Run nr23 0 deggres flowDiff was: -1
Run nr24 0 deggres flowDiff was: -4
Run nr25 0 deggres flowDiff was: -5
Run nr26 0 deggres flowDiff was: -2

Run nr27 0 deggres flowDiff was: 2
Run nr28 0 deggres flowDiff was: 0
Run nr29 0 deggres flowDiff was: 2
Run nr30 0 deggres flowDiff was: -5

LK Test 2 10d covered walls runs30

Run nr1 -10 deggres flowDiff was: 227
Run nr2 0 deggres flowDiff was: 10
Run nr3 0 deggres flowDiff was: 6
Run nr4 0 deggres flowDiff was: 7
Run nr5 0 deggres flowDiff was: 6
Run nr6 0 deggres flowDiff was: 9
Run nr7 0 deggres flowDiff was: 10
Run nr8 0 deggres flowDiff was: 8
Run nr9 -10 deggres flowDiff was: 165
Run nr10 -10 deggres flowDiff was: 208
Run nr11 0 deggres flowDiff was: 4
Run nr12 +10 deggres flowDiff was: -159
Run nr13 0 deggres flowDiff was: -10
Run nr14 0 deggres flowDiff was: -5
Run nr15 0 deggres flowDiff was: -4
Run nr16 0 deggres flowDiff was: -9
Run nr17 +10 deggres flowDiff was: -141
Run nr18 0 deggres flowDiff was: 4
Run nr19 0 deggres flowDiff was: -4
Run nr20 0 deggres flowDiff was: 10
Run nr21 0 deggres flowDiff was: 6
Run nr22 0 deggres flowDiff was: 10
Run nr23 0 deggres flowDiff was: 3
Run nr24 0 deggres flowDiff was: 6
Run nr25 -10 deggres flowDiff was: 172
Run nr26 -10 deggres flowDiff was: 173
Run nr27 0 deggres flowDiff was: 10
Run nr28 0 deggres flowDiff was: 0
Run nr29 0 deggres flowDiff was: 5
Run nr30 0 deggres flowDiff was: 4

LK Test 3 -10d covered walls runs50

Run nr1 0 deggres flowDiff was: -4
Run nr2 0 deggres flowDiff was: -7
Run nr3 0 deggres flowDiff was: -6
Run nr4 0 deggres flowDiff was: -7
Run nr5 +10 deggres flowDiff was: -188
Run nr6 0 deggres flowDiff was: -1
Run nr7 0 deggres flowDiff was: -1
Run nr8 0 deggres flowDiff was: 1
Run nr9 0 deggres flowDiff was: -5
Run nr10 +10 deggres flowDiff was: -176
Run nr11 0 deggres flowDiff was: 5
Run nr12 -10 deggres flowDiff was: 171
Run nr13 0 deggres flowDiff was: 6
Run nr14 0 deggres flowDiff was: -9
Run nr15 0 deggres flowDiff was: 0
Run nr16 0 deggres flowDiff was: -2
Run nr17 0 deggres flowDiff was: -2
Run nr18 0 deggres flowDiff was: -3
Run nr19 0 deggres flowDiff was: -8
Run nr20 +10 deggres flowDiff was: -57
Run nr21 0 deggres flowDiff was: -3
Run nr22 0 deggres flowDiff was: -1
Run nr23 0 deggres flowDiff was: 4
Run nr24 0 deggres flowDiff was: 7
Run nr25 0 deggres flowDiff was: 3
Run nr26 0 deggres flowDiff was: 3
Run nr27 0 deggres flowDiff was: 1
Run nr28 0 deggres flowDiff was: -3
Run nr29 0 deggres flowDiff was: -1
Run nr30 0 deggres flowDiff was: -5
Run nr31 0 deggres flowDiff was: 4
Run nr32 0 deggres flowDiff was: 2
Run nr33 0 deggres flowDiff was: 7
Run nr34 0 deggres flowDiff was: 0
Run nr35 0 deggres flowDiff was: 0
Run nr36 0 deggres flowDiff was: -1
Run nr37 0 deggres flowDiff was: -2
Run nr38 0 deggres flowDiff was: 4
Run nr39 0 deggres flowDiff was: 5
Run nr40 0 deggres flowDiff was: 3

Run nr41 0 deggres flowDiff was: -4
Run nr42 +10 deggres flowDiff was: -206
Run nr43 0 deggres flowDiff was: 6
Run nr44 0 deggres flowDiff was: -6
Run nr45 0 deggres flowDiff was: 9
Run nr46 -10 deggres flowDiff was: 165
Run nr47 -10 deggres flowDiff was: 145
Run nr48 -10 deggres flowDiff was: 118
Run nr49 +10 deggres flowDiff was: -266
Run nr50 +10 deggres flowDiff was: -172

LK Test 4 10d covered walls runs50

Run nr1 0 deggres flowDiff was: 7
Run nr2 -10 deggres flowDiff was: 218
Run nr3 -10 deggres flowDiff was: 171
Run nr4 -10 deggres flowDiff was: 181
Run nr5 0 deggres flowDiff was: -6
Run nr6 +10 deggres flowDiff was: -119
Run nr7 0 deggres flowDiff was: -3
Run nr8 0 deggres flowDiff was: -4
Run nr9 +10 deggres flowDiff was: -170
Run nr10 0 deggres flowDiff was: 9
Run nr11 -10 deggres flowDiff was: 149
Run nr12 0 deggres flowDiff was: -6
Run nr13 +10 deggres flowDiff was: -156
Run nr14 +10 deggres flowDiff was: -194
Run nr15 0 deggres flowDiff was: -6
Run nr16 0 deggres flowDiff was: 6
Run nr17 -10 deggres flowDiff was: 185
Run nr18 0 deggres flowDiff was: 5
Run nr19 0 deggres flowDiff was: -2
Run nr20 0 deggres flowDiff was: 4
Run nr21 0 deggres flowDiff was: 0
Run nr22 0 deggres flowDiff was: 1
Run nr23 0 deggres flowDiff was: -3
Run nr24 0 deggres flowDiff was: -7
Run nr25 0 deggres flowDiff was: -3
Run nr26 0 deggres flowDiff was: -8
Run nr27 0 deggres flowDiff was: -5

Run nr28 0 deggres flowDiff was: -3
Run nr29 0 deggres flowDiff was: 6
Run nr30 0 deggres flowDiff was: -1
Run nr31 +10 deggres flowDiff was: -175
Run nr32 +10 deggres flowDiff was: -197
Run nr33 +10 deggres flowDiff was: -186
Run nr34 0 deggres flowDiff was: 10
Run nr35 -10 deggres flowDiff was: 190
Run nr36 -10 deggres flowDiff was: 224
Run nr37 -10 deggres flowDiff was: 241
Run nr38 -10 deggres flowDiff was: 226
Run nr39 0 deggres flowDiff was: 6
Run nr40 0 deggres flowDiff was: -2
Run nr41 0 deggres flowDiff was: -3
Run nr42 0 deggres flowDiff was: -4
Run nr43 0 deggres flowDiff was: -5
Run nr44 0 deggres flowDiff was: -7
Run nr45 0 deggres flowDiff was: -9
Run nr46 0 deggres flowDiff was: -7
Run nr47 +10 deggres flowDiff was: -205
Run nr48 +10 deggres flowDiff was: -192
Run nr49 0 deggres flowDiff was: -2
Run nr50 0 deggres flowDiff was: -1

2nd Approach -10d whitewall runs10

Run nr1 -10 degrees right flow : 1678 left flow 4910 flow diff: -3232
Run nr2 -10 degrees right flow : 1503 left flow 4341 flow diff: -2838
Run nr3 0 degrees right flow: 3082 left flow: 3264 flow diff: -182
Run nr4 +10 degrees right flow: 8486 left flow 3048 flow diff : 5438
Run nr5 +10 degrees right flow: 6645 left flow 5483 flow diff : 1162
Run nr6 -10 degrees right flow : 4585 left flow 6319 flow diff: -1734
Run nr7 -10 degrees right flow : 6443 left flow 11044 flow diff: -4601
Run nr8 0 degrees right flow: 8429 left flow: 9223 flow diff: -794
Run nr9 +10 degrees right flow: 16852 left flow 9142 flow diff : 7710
Run nr10 -10 degrees right flow : 4725 left flow 8405 flow diff: -3680

2nd Approach 10d whitewall runs10

Run nr1 0 degrees right flow: 823 left flow: 1350 flow diff: -527
Run nr2 +10 degrees right flow: 9303 left flow 1916 flow diff : 7387
Run nr3 +10 degrees right flow: 3749 left flow 898 flow diff : 2851
Run nr4 +10 degrees right flow: 7620 left flow 2899 flow diff : 4721
Run nr5 +10 degrees right flow: 3328 left flow 2318 flow diff : 1010
Run nr6 -10 degrees right flow : 3771 left flow 4981 flow diff: -1210
Run nr7 -10 degrees right flow : 5197 left flow 7337 flow diff: -2140
Run nr8 -10 degrees right flow : 3053 left flow 11475 flow diff: -8422
Run nr9 -10 degrees right flow : 6213 left flow 13539 flow diff: -7326
Run nr10 -10 degrees right flow : 7840 left flow 10600 flow diff: -2760

2nd Approach -10d whitewall runs50

Run nr1 -10 degrees right flow : 732 left flow 3487 flow diff: -2755
Run nr2 -10 degrees right flow : 2521 left flow 4038 flow diff: -1517
Run nr3 -10 degrees right flow : 3259 left flow 5388 flow diff: -2129
Run nr4 0 degrees right flow: 3611 left flow: 4216 flow diff: -605
Run nr5 +10 degrees right flow: 7121 left flow 2934 flow diff : 4187
Run nr6 +10 degrees right flow: 12080 left flow 5512 flow diff : 6568
Run nr7 -10 degrees right flow : 4570 left flow 6900 flow diff: -2330
Run nr8 0 degrees right flow: 8893 left flow: 8966 flow diff: -73
Run nr9 0 degrees right flow: 8007 left flow: 8558 flow diff: -551
Run nr10 +10 degrees right flow: 7325 left flow 6212 flow diff : 1113
Run nr11 -10 degrees right flow : 6211 left flow 8230 flow diff: -2019
Run nr12 +10 degrees right flow: 7513 left flow 5703 flow diff : 1810
Run nr13 0 degrees right flow: 5007 left flow: 5087 flow diff: -80
Run nr14 +10 degrees right flow: 4407 left flow 1216 flow diff : 3191
Run nr15 +10 degrees right flow: 7750 left flow 2034 flow diff : 5716
Run nr16 -10 degrees right flow : 2039 left flow 5944 flow diff: -3905
Run nr17 -10 degrees right flow : 2128 left flow 11662 flow diff: -9534
Run nr18 -10 degrees right flow : 2449 left flow 13030 flow diff: -10581
Run nr19 -10 degrees right flow : 2743 left flow 8882 flow diff: -6139
Run nr20 +10 degrees right flow: 4565 left flow 2075 flow diff : 2490
Run nr21 +10 degrees right flow: 6128 left flow 4002 flow diff : 2126
Run nr22 0 degrees right flow: 6105 left flow: 6930 flow diff: -825
Run nr23 -10 degrees right flow : 2457 left flow 9495 flow diff: -7038
Run nr24 -10 degrees right flow : 1683 left flow 8744 flow diff: -7061
Run nr25 -10 degrees right flow : 4214 left flow 7533 flow diff: -3319
Run nr26 +10 degrees right flow: 3416 left flow 1335 flow diff : 2081
Run nr27 +10 degrees right flow: 5119 left flow 2300 flow diff : 2819

Run nr28 -10 degrees right flow : 2826 left flow 7440 flow diff: -4614
Run nr29 -10 degrees right flow : 1610 left flow 2724 flow diff: -1114
Run nr30 -10 degrees right flow : 2673 left flow 4438 flow diff: -1765
Run nr31 +10 degrees right flow: 6070 left flow 1275 flow diff : 4795
Run nr32 +10 degrees right flow: 16835 left flow 1289 flow diff : 15546
Run nr33 +10 degrees right flow: 19130 left flow 819 flow diff : 18311
Run nr34 0 degrees right flow: 905 left flow: 118 flow diff: 787
Run nr35 +10 degrees right flow: 9578 left flow 456 flow diff : 9122
Run nr36 +10 degrees right flow: 10253 left flow 478 flow diff : 9775
Run nr37 +10 degrees right flow: 10978 left flow 1787 flow diff : 9191
Run nr38 +10 degrees right flow: 7277 left flow 4526 flow diff : 2751
Run nr39 -10 degrees right flow : 5324 left flow 7233 flow diff: -1909
Run nr40 -10 degrees right flow : 4143 left flow 8226 flow diff: -4083
Run nr41 -10 degrees right flow : 4532 left flow 7905 flow diff: -3373
Run nr42 -10 degrees right flow : 4808 left flow 7243 flow diff: -2435
Run nr43 -10 degrees right flow : 3647 left flow 6054 flow diff: -2407
Run nr44 -10 degrees right flow : 3099 left flow 7931 flow diff: -4832
Run nr45 -10 degrees right flow : 4017 left flow 6953 flow diff: -2936
Run nr46 0 degrees right flow: 4569 left flow: 4206 flow diff: 363
Run nr47 +10 degrees right flow: 4129 left flow 1574 flow diff : 2555
Run nr48 +10 degrees right flow: 7022 left flow 1531 flow diff : 5491
Run nr49 +10 degrees right flow: 4574 left flow 1720 flow diff : 2854
Run nr50 +10 degrees right flow: 6026 left flow 1615 flow diff : 4411

2nd Approach 10d whitewall runs55

Run nr1 -10 degrees right flow : 277 left flow 2242 flow diff: -1965
Run nr2 +10 degrees right flow: 2184 left flow 439 flow diff : 1745
Run nr3 +10 degrees right flow: 4748 left flow 2101 flow diff : 2647
Run nr4 +10 degrees right flow: 8755 left flow 3720 flow diff : 5035
Run nr5 +10 degrees right flow: 9666 left flow 5209 flow diff : 4457
Run nr6 -10 degrees right flow : 4382 left flow 6638 flow diff: -2256
Run nr7 -10 degrees right flow : 5073 left flow 10268 flow diff: -5195
Run nr8 -10 degrees right flow : 5175 left flow 9469 flow diff: -4294
Run nr9 +10 degrees right flow: 6206 left flow 4763 flow diff : 1443
Run nr10 -10 degrees right flow : 3113 left flow 5317 flow diff: -2204
Run nr11 0 degrees right flow: 4172 left flow: 3472 flow diff: 700
Run nr12 0 degrees right flow: 3224 left flow: 2601 flow diff: 623
Run nr13 0 degrees right flow: 2003 left flow: 1717 flow diff: 286
Run nr14 +10 degrees right flow: 4679 left flow 2084 flow diff : 2595

Run nr15 -10 degrees right flow : 1003 left flow 3345 flow diff: -2342
Run nr16 +10 degrees right flow: 7938 left flow 4819 flow diff : 3119
Run nr17 +10 degrees right flow: 6676 left flow 5333 flow diff : 1343
Run nr18 -10 degrees right flow : 4024 left flow 5482 flow diff: -1458
Run nr19 -10 degrees right flow : 2310 left flow 4161 flow diff: -1851
Run nr20 +10 degrees right flow: 4128 left flow 1258 flow diff : 2870
Run nr21 +10 degrees right flow: 3898 left flow 2044 flow diff : 1854
Run nr22 0 degrees right flow: 4876 left flow: 5449 flow diff: -573
Run nr23 -10 degrees right flow : 1242 left flow 6567 flow diff: -5325
Run nr24 -10 degrees right flow : 1296 left flow 6710 flow diff: -5414
Run nr25 -10 degrees right flow : 773 left flow 3815 flow diff: -3042
Run nr26 +10 degrees right flow: 2193 left flow 382 flow diff : 1811
Run nr27 +10 degrees right flow: 3404 left flow 997 flow diff : 2407
Run nr28 0 degrees right flow: 4175 left flow: 3560 flow diff: 615
Run nr29 -10 degrees right flow : 237 left flow 2151 flow diff: -1914
Run nr30 0 degrees right flow: 812 left flow: 1656 flow diff: -844
Run nr31 +10 degrees right flow: 2663 left flow 1303 flow diff : 1360
Run nr32 -10 degrees right flow : 246 left flow 3468 flow diff: -3222
Run nr33 -10 degrees right flow : 21 left flow 1142 flow diff: -1121
Run nr34 0 degrees right flow: 733 left flow: 1730 flow diff: -997
Run nr35 0 degrees right flow: 8222 left flow: 8038 flow diff: 184
Run nr36 +10 degrees right flow: 7989 left flow 4000 flow diff : 3989
Run nr37 0 degrees right flow: 3444 left flow: 2527 flow diff: 917
Run nr38 0 degrees right flow: 2616 left flow: 3137 flow diff: -521
Run nr39 +10 degrees right flow: 2902 left flow 974 flow diff : 1928
Run nr40 +10 degrees right flow: 2398 left flow 76 flow diff : 2322
Run nr41 0 degrees right flow: 1549 left flow: 2021 flow diff: -472
Run nr42 -10 degrees right flow : 555 left flow 3865 flow diff: -3310
Run nr43 -10 degrees right flow : 758 left flow 6298 flow diff: -5540
Run nr44 -10 degrees right flow : 2676 left flow 6376 flow diff: -3700
Run nr45 0 degrees right flow: 2868 left flow: 3760 flow diff: -892
Run nr46 -10 degrees right flow : 1788 left flow 2919 flow diff: -1131
Run nr47 0 degrees right flow: 1638 left flow: 1617 flow diff: 21
Run nr48 +10 degrees right flow: 8068 left flow 1411 flow diff : 6657
Run nr49 +10 degrees right flow: 7934 left flow 2393 flow diff : 5541
Run nr50 +10 degrees right flow: 9931 left flow 288 flow diff : 9643
Run nr51 +10 degrees right flow: 3242 left flow 636 flow diff : 2606
Run nr52 -10 degrees right flow : 291 left flow 3090 flow diff: -2799
Run nr53 0 degrees right flow: 122 left flow: 576 flow diff: -454
Run nr54 +10 degrees right flow: 3851 left flow 411 flow diff : 3440
Run nr55 -10 degrees right flow : 302 left flow 1977 flow diff: -1675